Int J Adv Manuf Technol (2007) 31: 1135–1147
DOI 10.1007/s00170-005-0302-8

ORIGINAL ARTICLE

H. Ramasawmy · L. Blunt

Investigation of the effect of electrochemical polishing on EDM surfaces

Received: 23 March 2005 / Accepted: 15 July 2005 / Published online: 3 March 2006

Abstract Any surface generated by a manufacturing process bears a number of 'scars' due to the inherent nature of the process. In the electro discharge machining (EDM) process, the extremely high temperature generated, and the quenching effect of the dielectric at the end of each discharge lead to the formation of a hard and brittle white layer. It is important to remove the defects introduced by a manufacturing process so as to improve the functionality of the component/part. The aim of this work is to study the effect of parameters of electrochemical polishing on the 3D surface texture parameters of EDM surfaces of tool steel specimens. The results have shown a dominant effect due to the direct current of the cell, and there is a limiting value of the interelectrode gap for any given value of current density. A high influence of the interactive effect of current density and electrode gap was also observed. This information would be very useful in choosing the appropriate magnitude of the process parameters in order to engineer the surface to meet the in-service requirements, since the 3D surface texture parameters, particularly, the S_{ds}, S_{dr} and the volume parameters can give quantitative information with respect to the functionality of a surface, such as the load bearing and fluid retention capabilities as well as running in wear, etc.

Keywords Electrochemical polishing · Current density · Sodium nitrate · Electrode gap

H. Ramasawmy (✉)
Mechanical & Production Engineering Department,
University of Mauritius,
Reduit, Mauritius
e-mail: haree@uom.ac.mu

L. Blunt
School of Engineering & Computing,
University of Huddersfield,
Huddersfield, UK

Abbreviations J: Current density (A/cm^2) · S_a: Arithmetical average of the surface · S_q: Root-mean-square deviation of the surface · S_{ds}: Density of summits of the surface · S_{dr}: Developed interfacial area ratio · S_{ku}: Kurtosis of topography height distribution · S_{sk}: Skewness of topography height distribution · V_{mp}: Peak material volume of the surface · V_{mc}: Core material volume of the surface · V_{vc}: Core void volume of the surface · V_{vv}: Valley void volume of the surface

1 Introduction

The surface generated by the EDM process basically consists of randomly oriented peaks and valleys. Due to the high tensile stresses occurring during the process, localised fracture takes place on the surface; hence, cracks and micro-cracks appear on the EDM surface and high tensile residual stresses are inherent beneath the surface. Even with improved EDM technology it is very difficult to obtain a surface with low roughness value, free from imperfections such as blow holes, pock marks and cracks, and free from tensile residual stresses.

Several researchers, namely, McGeough et al. [1], and Sakai et al. [2], have developed hybrid machines combining EDM and ECM (electrochemical machining) in order to improve the EDM surface. They have obtained good results but the system is quite complicated and requires a high level of control.

Other researchers, namely, Boza [3], have tried to polish the EDM surface with an electrochemical polishing (ECP) process. ECP is a low-level electrochemical dissolution process in which the tool is the cathode and the workpiece is the anode in an electrolytic cell. There is no physical contact between the workpiece and the tool. The temperature developed is too low to cause any phase transformation of the material. In addition, there is no risk of induced tensile residual stresses. Literature [4, 5] shows evidence of a direct relationship between occurrence of tensile residual stresses and decrease in fatigue strength. An EDM surface treated by

ECP would have a better fatigue endurance limit than the EDM surface.

Most of the ECP research work performed on steel have used a mixture of acids. Moreover, there is no proper 3D surface characterisation of electrochemically polished EDM surface in order to assess the functional capabilities of the treated surfaces under different ECP conditions.

The main objective of this paper is to present the findings of experimental work in assessing the influence of ECP process parameters on 3D surface texture parameters, and relate the findings to the physical principle of the process.

2 Literature review

2.1 ECP process

Electrochemical polishing (ECP) is an anodic dissolution process using an electrochemical reaction. It can produce a smooth, bright, and reflective surface that exhibits superior corrosion resistance when the workpiece (anode) and tool electrode (cathode) are electrically coupled. Both tool and workpiece are immersed in a suitable electrolyte and a potential difference of 2 to 20 V DC is normally applied across the electrodes whereby the material is removed from the anode by the electrolytic action (Fig. 1). The material removed from the anode and the hydrogen gas liberated at the cathode are swept away by the electrolyte. Concerning the magnitude of current to use, as a rule of thumb, it is recommended to provide 0.004 m^3 of bath for each 2–4 amp of current to be passed in electrolyte at 65.5–93.3°C [4].

Electrochemical polishing is suitable for the polishing of both complex shapes and hardened materials, which are difficult to machine mechanically because in ECP the electrode and the workpiece are not in contact with each other. The mechanism of ECP is not yet fully clear, but it is usually explained as follows: an electrochemical polishing effect occurs because of differential dissolution, as the current is applied, the oxidation film covering the lower peaks of the surface, which has a high specific gravity, viscosity, and insulation, prevents dissolution, while the higher peaks uncovered with the oxidation film, which receive greater current from the cathode, dissolve more quickly. Since the ECP process, by nature, is a metal dissolution process, each of the peaks that protrudes into the anode film will have a significantly greater charge concentration on them than on the valleys of the workpiece, and thus will be removed faster than the valleys of the material's surface [6].

ECP removes materials from the surface of the metal selectively, for example, electrochemical polishing does not readily remove carbon from a metal because carbon is electrochemically passive. The chromium and nickel in stainless steel become uncovered and remain on the surface of the metal as a result of ECP. Large quantities of chromium react with the oxygen of the process to form chromium oxides, while nickel, chromium, iron and carbon combine to form nichrome. In this reaction, at least some of the carbon is used in the formation of nichrome and chromium oxides. Because ECP creates these chromium oxides, a 15 to 20 times increase in corrosion resistance can be expected in electrochemically polished parts made with these types of material [6].

2.2 Effect of ECP process parameters

2.2.1 Electrode gap and current density

Most of the existing literature [3, 6, 7] of ECP on steel surfaces deals with the use of acidic electrolyte rather than salts. Important parameters in ECP are current density, electrode gap, temperature of the electrolyte, type of electrolyte, and flow rate. Their influences are detailed below.

Lee [6], with an acidic electrolyte and electrode gap of 1 mm, found that in ECP of stainless steel a high current density (above a critical value) leads to reduction in the surface roughness. He also determined that an appropriate polishing time should be chosen since continuous improvement of the workpiece surface cannot be expected beyond a critical value. The surface roughness also decreased as the electrolyte temperature was increased, and 68°C was found to be optimum. In cases where the electrolyte temperature

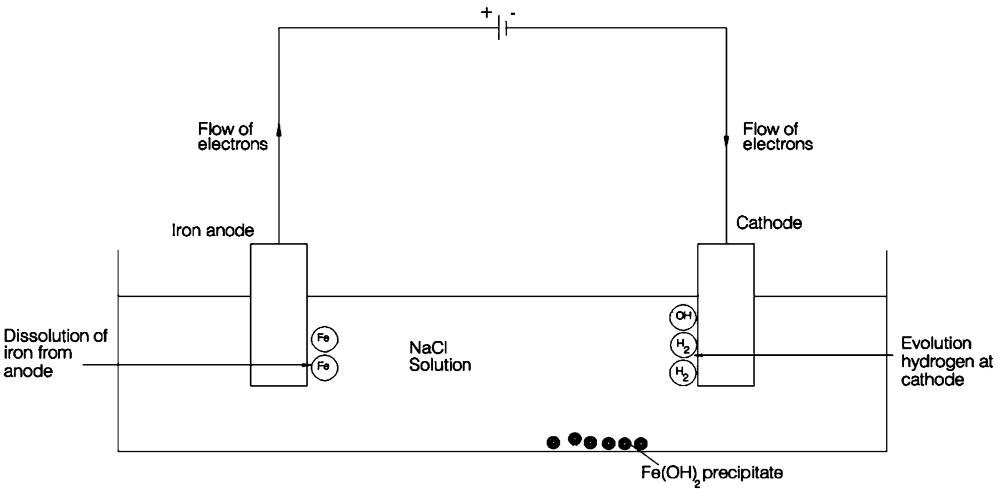

Fig. 1 Dissolution process due to the ECP process

increases, the ECP effect becomes more active with high current efficiency caused by the low viscosity and increased specific conductivity of the electrolyte. This process promotes selective dissolution with an oxide film covering the lower peaks on the surface, and consequently the process produces excellent results in a short time.

In general the surface roughness of the workpiece decreases as the electrode gap is reduced. In the case of a narrow electrode gap, it is observed that more pits are formed at an electrode gap of 0.5 mm than for one of 1.0 mm. Generally, pits can be formed at a certain small spot where a high current density is applied in the case of a narrow electrode gap. Certain conditions may even lead to sparking [6]. Consequently, an appropriate electrode gap must be selected while performing ECP. Because the ECP process has a limited ability to improve surface roughness, it must be taken into account that the surface roughness before ECP influences the quality of the final ECP surface. Lee reported that the electrochemical polishing effect can be obtained quickly when a current density of at least greater than 8 A/cm^2 is applied [6].

Many researchers [2, 8] have used a very high amperage with a pulsed generator for their electrochemical experiments, where the electrochemical process is being used as a finishing process, and they have used very small electrode gaps (typically less than 1 mm). Boza [3] proposed a gap distance of more than 1 mm for ECP.

2.2.2 *Effect of electrolyte and its flow rate*

Boza [3] has used acidic electrolytes to ECP spark eroded steel samples. A mixture of phosphoric, sulphuric, and chromic acid in water at 80°C proved effective. He then used this electrolyte for the ECP of real steel tools. He reported a 50% decrease in the R_t and R_q surface roughness parameters, but noted that this is limited by the presence of complex carbide grains. Since these carbides do not dissolve easily as compared to the steel matrix, they remain on the surface of the tool. He found that there has been a 40–50% increase in the tool life after the ECP process as compared to a ground tool.

Boza [3] also recommends the use of stagnant electrolyte for ECP. However, Rajurkar and Schnacker [8] have observed that the higher the flow rate of the electrolyte, the smoother is the workpiece surface. They observed that the higher electrolyte flow rate removes hydrogen bubbles more effectively from the cathodic grooves resulting in an increased local ionic strength and, therefore, more effective metal removal on the anode. Masuzawa and Sakai [9] have used flow rates of 750 ml/min when polishing a surface by the electrochemical process. They further reported that lustrous surfaces could be obtained with a 25% (by wt) sodium nitrate solution at a flow rate of 250 ml/min. They also observed a black smooth surface at 100 ml/min. In a later paper, Sakai et al. [2] reported their findings on the polishing of die sink EDM surfaces by the electrochemical process. In this case they used sodium nitrate solution at a high current density (30 A/cm^2). In one case, the electrolyte was flowing during the pulsed current, and in another case the electrolyte was stagnant. They observed 1–2 μm difference (in favour of flowing electrolyte) in the roughness of surfaces between stagnant and flowing electrolyte processes.

From the above discussion, it is essential to investigate the polishing effect of salt electrolytes under conditions of low current density and wide electrode gap (larger than 1 mm).

3 Methodology

In order to perform the ECP tests, a standard EDM surface had to be produced. The magnitude of the selected 3D surface texture parameters for the base EDM surface are as follows: S_q=22.80 μm, S_{sk}=0.19, S_{ku}=2.89, S_{ds}=96.43 mm^{-2}, S_{dr}=10.27%, V_{mp}= 1.13E+06 μm^3/mm^2, V_{mc}=2.11E+07 μm^3/mm^2, V_{vc}=2.83E+07 μm^3/mm^2, V_{vv}=2.15E+06 μm^3/mm^2. The ECP process time was set at 5 min. Thus a peak current value of 22.35 A and a pulse duration of 500 μs as well as an OFF time of 100 μs were used on the spark erosion machine. The EDM surface area was set at 25 mm × 25 mm. Prior to the EDM machining each specimen was ground (to provide flat surfaces) and annealed in order to remove any residual stresses due to the preceding operations. The material used for the experiments was M300 (0.38% C, 0.40% Si, 0.65% Mn, 16.00% Cr, 1.00% Mo, and 0.80% Ni) stainless martensitic chromium tool steel from Bohler (South Africa). Commercial copper (25 mm × 25 mm) was used as the cathode.

Based on the findings of Masuzawa and Sakai [9], and on previous trial runs, it was noted that sodium nitrate solution gave satisfactory polishing results during an ECP process. This electrolyte solution presents less safety hazards and is cheaper as compared to the usual solution mixture of sulphuric and phosphoric acids used in electrochemical polishing of stainless steels. Thus, the 50% sodium nitrate solution was used as the electrolyte for both preliminary and final ECP sets of experiments.

3.1 Preliminary set of experiments for ECP

Based on literature review, three factors, namely, direct current, electrode gap and electrolyte flow rate, were found to be important variables during the electrochemical polishing process. A preliminary design of experiments using the orthogonal array (OA) was carried out in order to assess the relative effect of these three ECP parameters. Four levels of each factor were used in the design through an L16 orthogonal array. Table 1 shows the matrix of process conditions used in the experimentation.

With reference to literature [3, 4] it has been shown that for ECP, low current densities are normally used since the main objective is not for high stock removal but surface smoothing. Following the trial runs that were done at a maximum direct current density of 0.48 A/cm^2, it was observed that a significant amount of polishing occurred in a relatively short time span (6 min). But in order to observe the polishing effect at higher current density, a maximum

Table 1 L16 OA for the preliminary ECP experimental set

Trial	Current density, A/cm^2	Flow rate, ml/min	Electrode gap, mm
1	0.16	0	1.5
2	0.16	218	10
3	0.16	574	25
4	0.16	814	40
5	0.48	0	10
6	0.48	218	1.5
7	0.48	574	40
8	0.48	814	25
9	0.8	0	25
10	0.8	218	40
11	0.8	574	1.5
12	0.8	814	10
13	1.28	0	40
14	1.28	218	25
15	1.28	574	10
16	1.28	814	1.5

value of 1.28 A/cm^2 was chosen. A continuous direct current source was used, and larger electrode gaps were selected. For the sake of the experiments, a minimum of 1.5 mm and a maximum of 40 mm electrode gap distances were used.

Given the findings from Sect. 2.2.2, three different magnitudes of electrolyte flow rate (218, 574 and 814 ml/min) and one level without re-circulation were used in the preliminary experiments.

3.2 Final design of experiments for ECP

Based on the ANOVA results of a preliminary set of ECP experiments of the 3D surface texture measurements (see Sect. 5.1), a final design of experiments (DoE) was conducted with only the two dominant controllable factors (current and electrode gap distance). This finding (the dominant effect of the current and electrode gap factors) seems to be in line with the observation from Boza [3]. Due to limitations of the power supply equipment a maximum value of 1.76 A/cm^2 current density was used. It was decided to use five levels of the two factors in order to maximise data collection for a proper mathematical correlation. A full factorial design of experiments with two factors (twenty-five experiments) was used. Thus for the final ECP experiments the five levels of current densities used were 0.16, 0.48, 0.8, 1.28 and 1.76 A/cm^2, and the five levels of electrode gap were 1.5, 10, 20, 40, and 60 mm.

For each experiment during the final set, the electrolyte was maintained at pH in the range of 8.5 to 8.9, and the temperature was in the range 21.75°C to 24.5°C. A stagnant electrolyte condition was maintained.

4 Surface texture measurements

Control of surface roughness is carried out for a myriad of functional reasons as diverse as printability to fluid flow. However, the primary reasons for investing in production of a functional surface are to reduce the initial wear of parts that are in contact, to improve the fatigue resistance (surface irregularities are the seat of fatigue failure), to allow fine geometric and dimensional tolerance to be held (this cannot be done if the surfaces involved have irregularities that are nearly as large as the tolerance allowed on their positions), to reduce frictional wear (smooth contacting surfaces will wear less rapidly than rough surfaces), to reduce corrosion by minimising the number and depth of crevices where corrosion proceeds at a high rate, and to improve lubrication by "engineering" lubrication reservoirs.

This does not imply that a perfectly smooth surface is always ideal; for example, a controlled degree of roughness is usually required in a cylinder bore to allow 'reservoirs' of oil to be present. However well two surfaces in relative motion (e.g. a shaft and its bearing) are lubricated, some wear will occur. If the surfaces are rough they will soon become smoother as the peaks wear away. The result of the material removal will be a quicker change in the fit of the two parts than if the surface finish was at the optimum to start

Table 2 ANOVA analysis for the 3D parameters based on the preliminary set of electrochemical polishing tests

	Current density	Flow rate	Elec gap		Current density	Flow rate	Elec gap
3D parameter	% *SSA*	% *SSB*	% *SSC*	% *SSe*	F_a	F_b	F_c
S_q (μm)	24.91	20.69	27.80	26.60	11.86	9.85	13.24
S_z (μm)	17.78	12.85	33.13	36.25	6.21	4.49	11.58
S_{ds} (1/mm^2)	34.74	12.74	31.85	20.67	21.28	7.81	19.51
S_{dr} (%)	15.38	30.64	15.97	38.01	5.13	10.21	5.32
V_{mp} (μm^3/mm^2)	3.42	29.47	13.38	53.74	0.81	6.95	3.15
V_{mc} (μm^3/mm^2)	35.04	19.86	22.86	22.25	19.95	11.30	13.02
V_{vc} (μm^3/mm^2)	11.99	25.26	26.29	36.47	4.16	8.77	9.13
V_{vv} (μm^3/mm^2)	48.76	4.99	25.78	20.47	30.17	3.09	15.95
S_{pk} (μm)	4.34	27.94	13.27	54.45	1.01	6.50	3.09
S_k (μm)	40.54	18.08	20.29	21.09	24.35	10.86	12.19
S_a (μm)	26.70	22.06	25.58	25.66	13.18	10.89	12.63
S_{5z} (μm)	20.87	13.77	28.19	37.17	7.11	4.69	9.60

Table 3 ANOVA analysis for 3D parameters based on the final set of electrochemical polishing tests

	Current density (A)	Electrode gap (B)	Interactive effect	Error	Current density (A)	Electrode gap (B)	Interactive effect
3D parameter	% *SSA*	% *SSB*	% *SSAB*	% *SSe*	F_a	F_b	F_{ab}
S_q (μm)	55.52	10.01	20.46	14.01	49.52	8.93	4.56
S_z (μm)	36.77	17.46	20.73	25.04	18.35	8.71	2.59
S_{ds} (1/mm^2)	51.30	24.21	13.85	10.63	60.33	28.47	4.07
S_{dr} (%)	28.78	1.38	43.60	26.24	13.71	0.66	5.19
V_{mp} (μm^3/mm^2)	4.11	4.63	54.93	36.33	1.41	1.59	4.72
V_{mc} (μm^3/mm^2)	64.11	8.18	15.78	11.93	67.16	8.57	4.13
V_{vc} (μm^3/mm^2)	43.21	8.70	27.41	20.69	26.11	5.25	4.14
V_{vv} (μm^3/mm^2)	69.18	9.50	7.91	13.41	64.48	8.85	1.84
S_{pk} (μm)	2.12	5.70	56.89	35.30	0.75	2.02	5.04
S_k (μm)	67.85	7.71	13.80	10.64	79.71	9.06	4.05
S_a (μm)	58.22	9.13	18.87	13.78	52.80	8.28	4.28
S_{5z} (μm)	42.90	13.90	23.46	19.74	27.17	8.80	3.71

with. On the other hand some parts such as clamping devices or a pin with an interference fit depend on friction for their functionality.

Another application where surface finish can have an influence on performance is the use of lip seals to prevent the escape of hydraulic fluids. If the finish is too smooth it is difficult to maintain a fluid film between the shaft and the seal. If the finish is too rough it can cause abrasion and consequent breakdown leading to failure.

With the above examples, it can be seen how important surface texture is. We can appreciate the fact that the mere specification of the peak to valley height (R_t) or the arithmetic mean roughness value (R_a) is not sufficient in defining entirely the micro-geometry of a surface.

A number of case studies have been presented by Blunt and colleagues [10–14] ranging from automotive engine performance to functionality of bio implants where the advantages of measuring surfaces in 3D have been demonstrated. They conclusively showed clearer understanding of functionality when 3D surface metrology was employed.

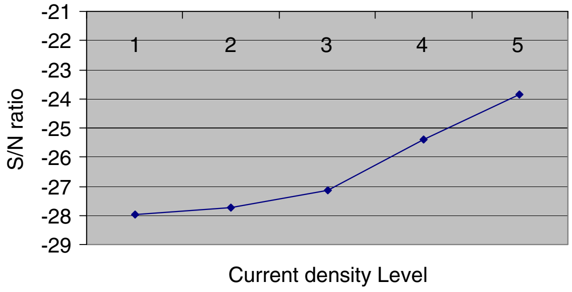

Fig. 2 Influence of current density on the S/ N ratio of S_q

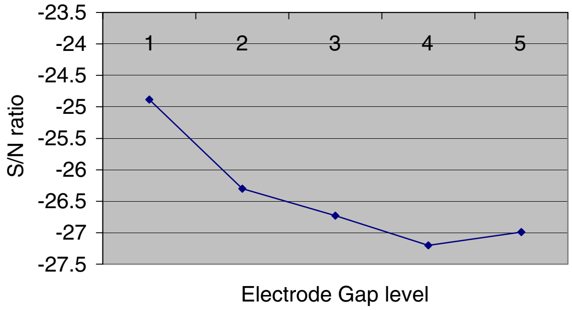

Fig. 3 Influence of electrode gap on S/N ratio of S_q

This calls for a better knowledge of the influence of the production process parameters on the generation of the micro-geometry of a surface. This leads us to the actual three-dimensional aspects of surfaces, i.e. how the micro-geometry is defined in terms of amplitudes, spatial, and volumetric functions.

Some of the important 3D surface texture parameters [15] that have been used in this paper are defined in the list of abbreviations.

3D surface texture measurements were carried out using a Talysurf Form 2 Series instrument (Taylor-Hobson, UK). A 60° conical diamond stylus of 2 μm tip radius was used for all measurements. The measuring area was set at 4 mm × 4 mm and the *y*-axis interval was 8 μm. The number of data points collected per trace amounted to 1,024. For each specimen, three measurements were performed at different locations on the workpiece's surface. The average value was then computed and used for the different analyses. Subsequent analysis was made using

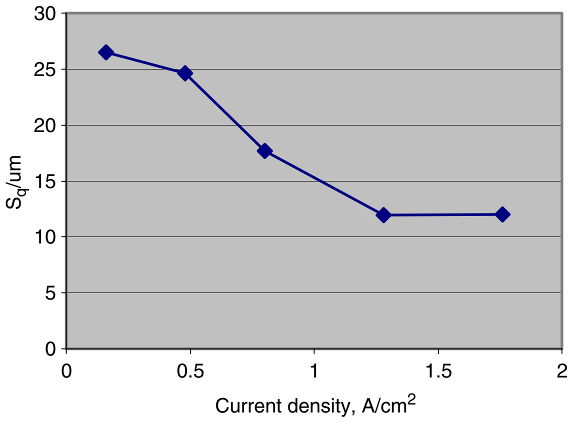

Fig. 4 Trends of S_q with current density at an electrode gap of 1.5 mm

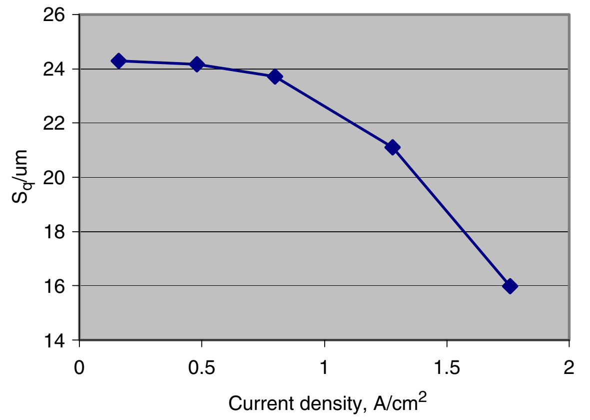

Fig. 5 Trends of S_q with current density at an electrode gap of 20 mm

the 3D surface characterisation software package developed at the University of Huddersfield (UK) as part of an EC project called SURFSTAND. It should be noted that all the raw surface texture data were not filtered by the software. It was thought that since the roughness value for the different experiments would not be less than 1 µm, filtering should be avoided as it might remove some important data.

5 Results and analysis

5.1 Preliminary ECP tests

The results of the ANOVA analysis for the selected 3D surface roughness parameters based on the preliminary set of electrochemical polishing effects are shown in Table 2. It is observed that for the amplitude parameters, S_{ds}, V_{mc} and V_{vv}, the effects due to the electrode gap and current density are higher as compared to that of flow rate. However, the percentage contribution of flow rate is higher than the current density effect for the parameters S_{dr}, V_{mp}, V_{vc}, and S_{pk}. V_{mp} and S_{pk} represent the extreme surface texture definition in their respective category. Basically, these two parameters represent the extreme top points on the sampling area. Since a change in the flow rate has a large bearing on film thickness at the peaks, it is likely to affect the extreme points of the asperities as well as the core part of the craters.

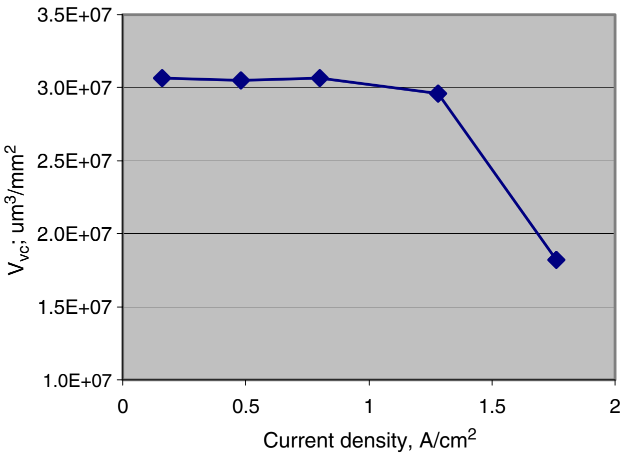

Fig. 7 Trends of V_{vc} with current density at an electrode gap of 20 mm

But it should be noted that for all surface texture parameters (except for V_{vv}) the percent contribution of the flow rate is within 10% and 30% indicating its effect on the surface texture. The very low value of the effect of flow rate on V_{vv} can be explained by the fact that this parameter provides a quantitative assessment of the bottom part of the valley, and this region will be the last to be affected by the polishing effect. Films are normally formed during the process and the type of film formation depends on the metal, electrolyte used, and the process conditions. The thickness of film is considerably lower on peaks and higher at valleys. Hence polishing of valleys would be lower.

The percentage contribution due to errors (SSe) is quite high for all surface texture parameters (20%<SSe>40%), and in the case of the extreme parameters, namely, peak material volume and S_{pk}, the error is 50% to 55%. It is

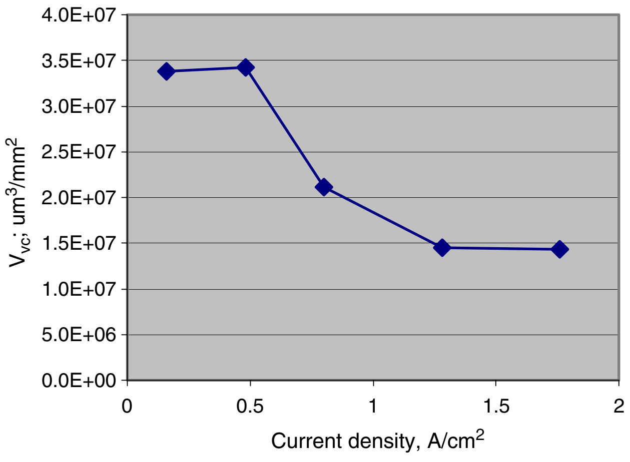

Fig. 6 Trends of V_{vc} with current density at an electrode gap of 1.5 mm

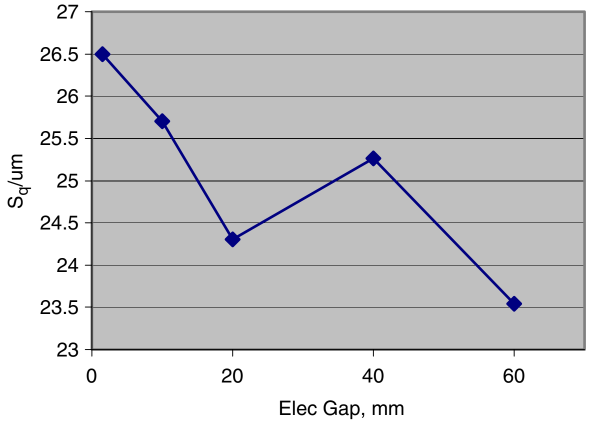

Fig. 8 Trends of S_q with electrode gap at current density of 0.16 A/cm^2

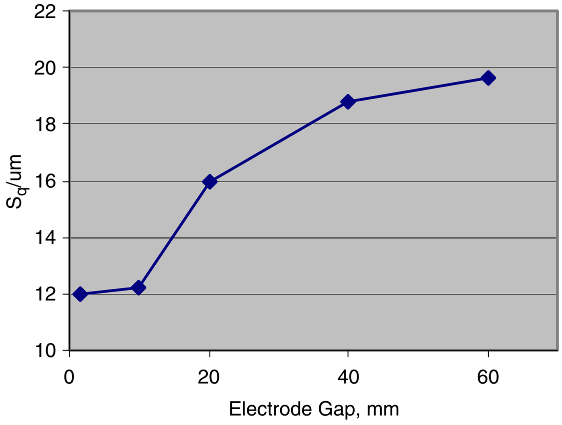

Fig. 9 Trends of S_q with electrode gap at current density of 1.76 A/cm^2

noted that SSe represents the combination of interaction effects among the three process factors as well as avoidable and uncontrollable error sources. Temperature was in the range of 21–27°C, which could influence the dissolution of the metal. The pH was also observed to increase steadily from a value of 7.2 for the first preliminary experiment (ECP1) to 9.5 for the last one (ECP16). This increase in the pH could affect the rate at which metal atoms dissolve as ions in the electrolyte, especially bearing in mind that the pH is a logarithmic scale.

5.2 Final ECP experiments

5.2.1 3D surface texture measurements

The results of the ANOVA analysis for the selected 3D parameters are shown in Table 3. From this data, it is observed that for all the amplitude surface texture parameters (S_q, S_a, S_{5z}, S_z), S_{ds}, V_{mc}, V_{vc}, V_{vv}, and S_k, the effect of current density is much higher as compared to that of the electrode gap and of the interaction effect of both factors. However, the percentage contribution of the interactive effect (43.6%) of current density and electrode gap is more important than the individual effect of current (28.8%) for S_{dr}. The effect of electrode gap is slightly higher than that of current density for only the V_{mp} and S_{pk} parameters. But for these two surface texture parameters, the percentage contribution of the interaction effect is above 50%, and that of the error is high (about 35%). The very high F values for the current density factor (except for V_{mp} and S_{pk}) and for electrode gap (except for S_{dr}, V_{mp} and S_{pk}) for all the selected 3D surface texture parameters indicate high reliability as compared to the percentage error.

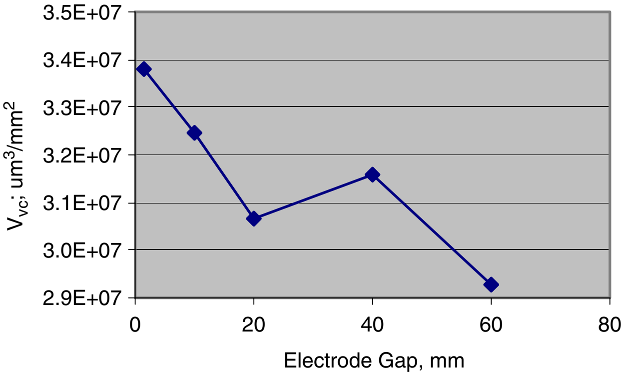

Fig. 10 Trends of V_{vc} with electrode gap at current density of 0.16 A/cm^2

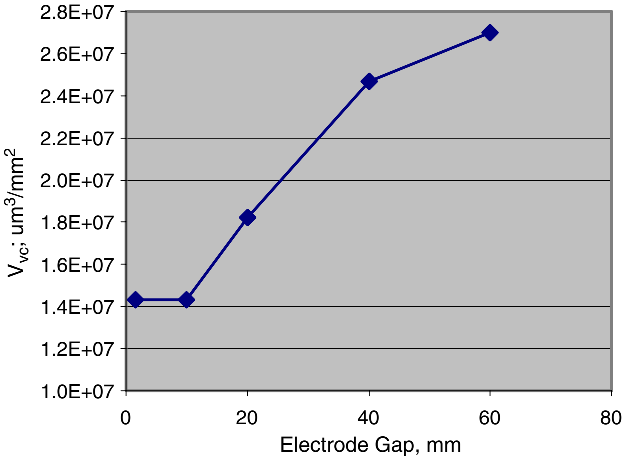

Fig. 11 Trends of V_{vc} with electrode gap at current density of 1.76 A/cm^2

The high contribution of the interaction of the two factors clearly shows that the rate of dissolution is very much dependent on the path length of the ion migration in solution in order to cause the ionic process.

Calculation of the signal to noise (S/N) ratio for the S_q parameter shows that there is an improvement in this amplitude parameter as the current density is increased and the electrode gap is reduced (Figs. 2 and 3).

The trends of S_q and V_{vc} with current density at gap sizes of 1.5 and 20 mm are shown in Figs. 4, 5, 6 and 7. At a gap of 1.5 mm it can be observed that the surface texture in terms of the root mean surface height as well as the core volume of the EDM craters is improving as the current

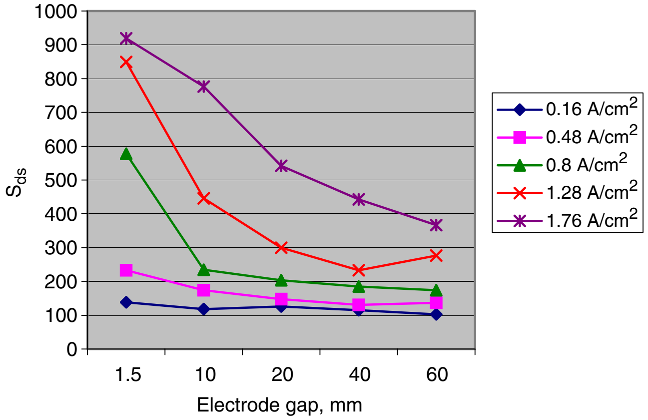

Fig. 12 The variation of density of summits (S_{ds}) with electrode gap at different current density levels

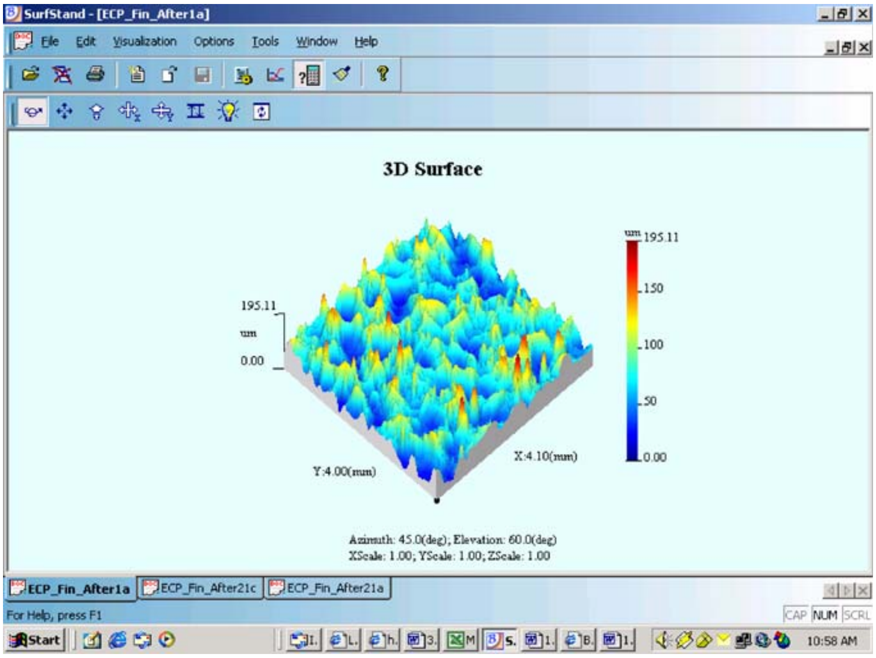

Fig. 13 3D axonometric plot of the ECP surface with an electrode gap of 1.5 mm at 0.16 A/cm^2

density is increased from 0.16 A/cm^2 to 1.28 A/cm^2. It is observed that when a narrow gap of 1.5 mm is used, a sharp drop in the S_q (by 54%) and V_{vc} (by 57%) parameters occurs at 0.8 A/cm^2. On the other hand, at a gap of 20 mm, a reduction of 2.4% in the S_q and 0.11% in the V_{vc} occurs at 0.8 A/cm^2. These values reveal that for a given value of current density different phenomena are occurring when the electrode gap is changed. For a given value of current density, as the electrode gap is reduced from a high value to a limiting condition, the polishing process appears to take over the etching action.

The trends of S_q and V_{vc} with electrode gap at current densities of 0.16 A/cm^2 and 1.76 A/cm^2 are shown in Figs. 8, 9, 10 and 11. At 0.16 A/cm^2 there is negligible effect irrespective of the gap size since it is believed that the current density level is too low to initiate a significant polishing effect. The apparent decrease in the S_q and V_{vc} values (Figs. 8 and 10) should not be interpreted as a smoothing action but rather due to the variation of the surface texture value over the surface of the measured specimens. However, at a current density of 1.76 A/cm^2 a clear improvement is seen at the narrow gap of 1.5 mm and

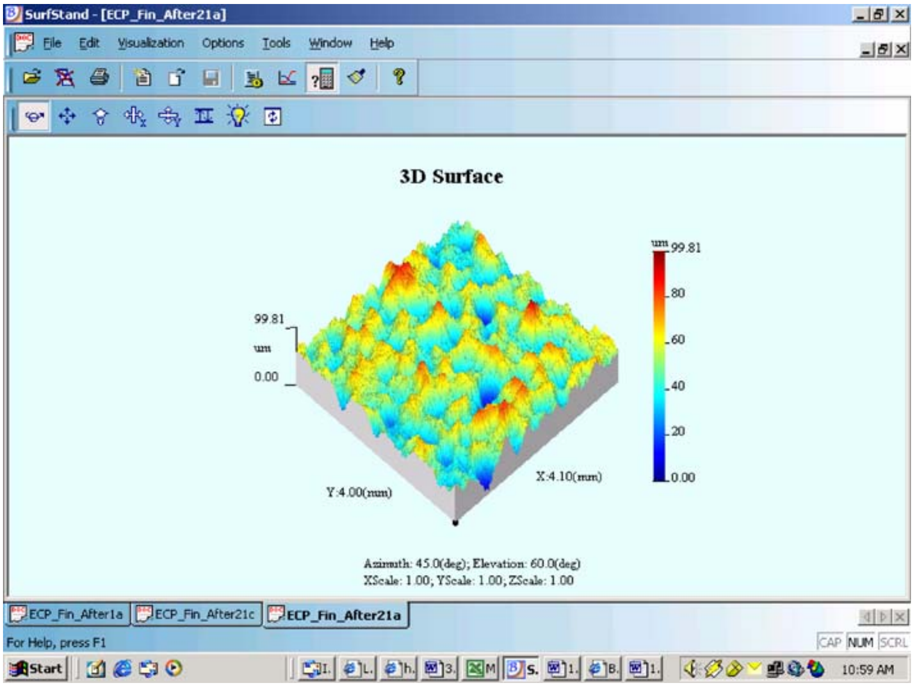

Fig. 14 3D axonometric plot of the ECP surface with an electrode gap of 1.5 mm at 1.76 A/cm^2

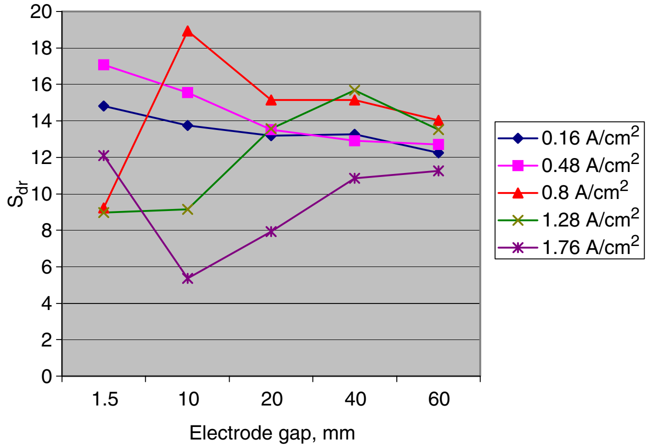

Fig. 15 The variation of S_{dr} with electrode gap at different current density levels

even at 10 mm. In fact at this particular level of current density the difference in the volume and amplitude parameters between the 1.5 mm and 10 mm electrode gap levels is very small and almost negligible. This observation tends to reveal that for a given current density level there is an optimum level of the electrode gap below which no further improvement in the surface texture parameters can be obtained.

Figure 12 shows the variation of density of summits (S_{ds}) with electrode gap at different current density levels. The highest value for the S_{ds} parameter occurs at the highest current density and at the lowest electrode gap; and at the relatively high current density level (J>0.48 A/cm^2), there is a significant decrease (more than 40%) in S_{ds} as electrode gap increases from 1.5 mm to 20 mm. For the low current density levels (0.16 A/cm^2 and 0.48 A/cm^2), a slight decrease is observed from 1.5 mm to 10 mm, and almost no variation with larger gap. The graph shows that even at the larger gap (60 mm) significant polishing is taking place when the current density is 1.76 A/cm^2. This is evident from the value of S_{ds} which stands at 366.67 and that the base EDM surface had an S_{ds} value of 96.43. Whereas at low current density (0.16 A/cm^2) the S_{ds} value is 138.33 with an electrode gap of 1.5 mm. This would tend to suggest that a different phenomenon is taking place when the current density and electrode gap conditions are different. The high values of S_{ds} for the high current density conditions at relatively small electrode gap tend to indicate that there are more summits above the least square plane as compared to low current density conditions (at relatively small electrode gap). Hence this would suggest better load bearing capabilities of the surface. In general it is observed that the highest dissolution brings about an increase in number of summits, i.e. a significant reduction in the standard deviation of the peak height. This shows that at high current density and small electrode gap conditions, the few protruding (high S_q) peaks get dissolved and flatten out. Figures 13 and 14 show the 3D axonometric plots of the ECP surfaces with an electrode gap of 1.5 mm at 0.16 A/cm^2 and 1.76 A/cm^2, respectively. It can be seen that the surface at 0.16 A/cm^2 is more spiky, and has a few high peaks as compared to the surface at the higher current density.

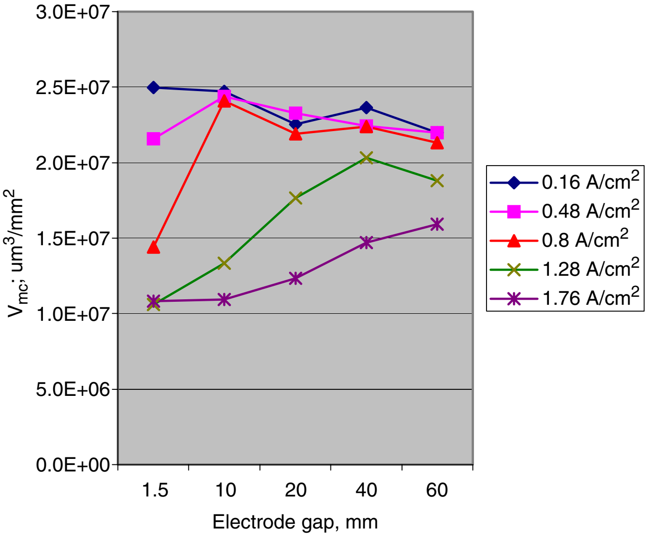

Fig. 17 The variation of the core material volume parameter with electrode gap at different current density levels

Fig. 16 The variation of the peak material volume parameter with electrode gap at different current density levels

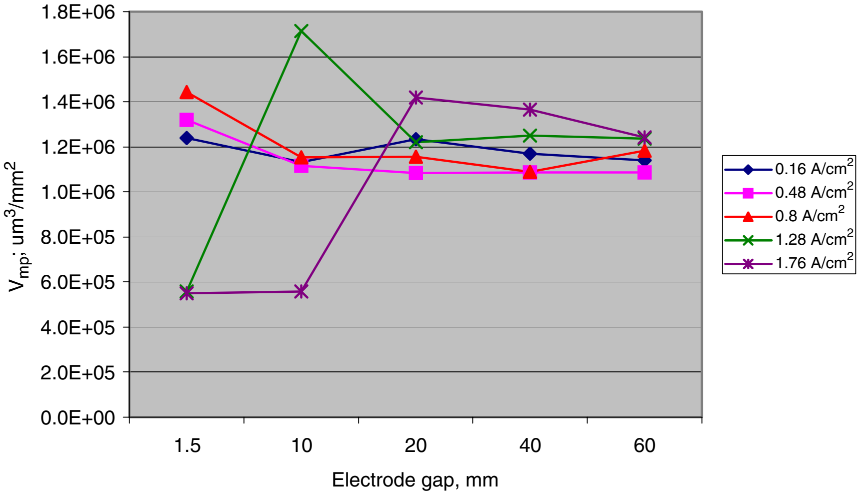

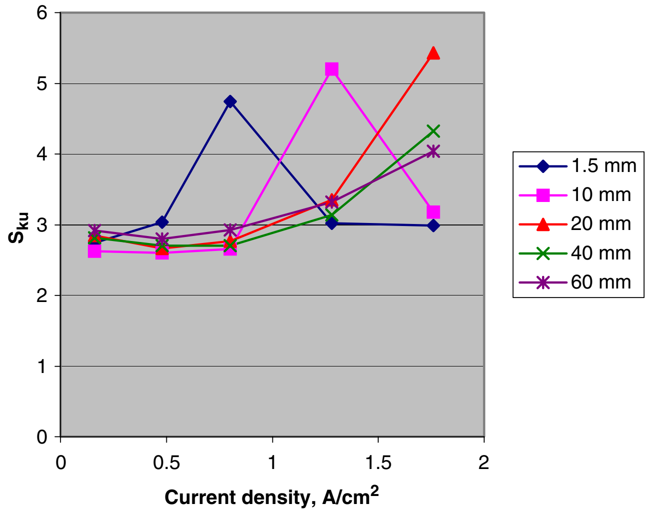

Fig. 18 Trends of S_{ku} with current density at different electrode gap levels

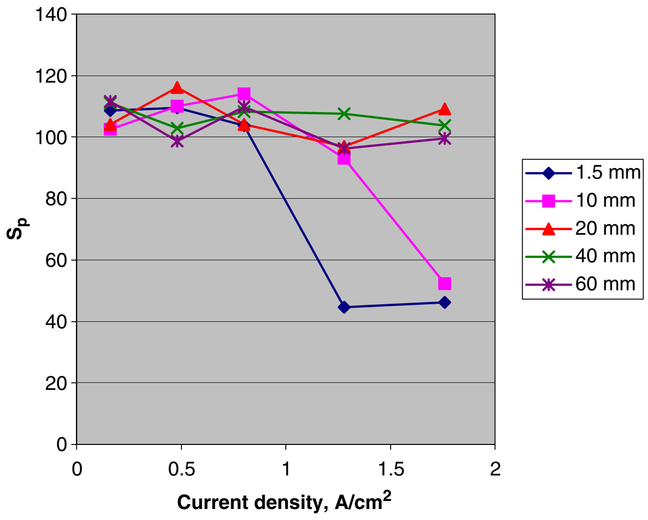

Fig. 20 Trends of S_p with current density at different electrode gap levels

Since the position of the least square plane is also lowered on account of an overall reduction in the amplitude parameters (S_q, S_a), a larger proportion of the shorter peaks would be above the least square plane. Hence, this accounts for an increase in the S_{ds} parameter. Since there are more summits, and the standard deviation of the height of summits would be smaller, this would then result in a better dimensional fit of mating surfaces after the initial running in period.

Figure 15 shows the variation of S_{dr} with electrode gap at different current density levels. For the higher value of current density, the variation in the developed interfacial area ratio (S_{dr}) at the small gap is almost double that at the larger gap, but at smaller current density levels, the difference is less significant. This phenomenon confirms the significant change of the density of summits at higher current density levels as compared to the changes at lower current density values. Moreover, for the higher current density conditions (for 1.28 A/cm^2 and 1.76 A/cm^2), there is an increase in the S_{dr} from electrode gap 10 mm to 60 mm. This tends to support the statement regarding the decrease in the density of summits (S_{ds}) when the electrode gap is increased. This means that there are less summits at the wider electrode gap having long slanting surfaces, that is, the developed interfacial area is high. Also, the numerous summits at the narrower electrode gap (under high current conditions) are shorter in height, that is, they have a smaller value of developed interfacial area. Thus the risk of high initial running in wear (for the surfaces in service) is lower for the conditions of high current density and narrow electrode gap.

Figures 16 and 17 show the variation of the peak (V_{mp}) and core (V_{mc}) material volume parameters, respectively, with electrode gap at different current density levels. For

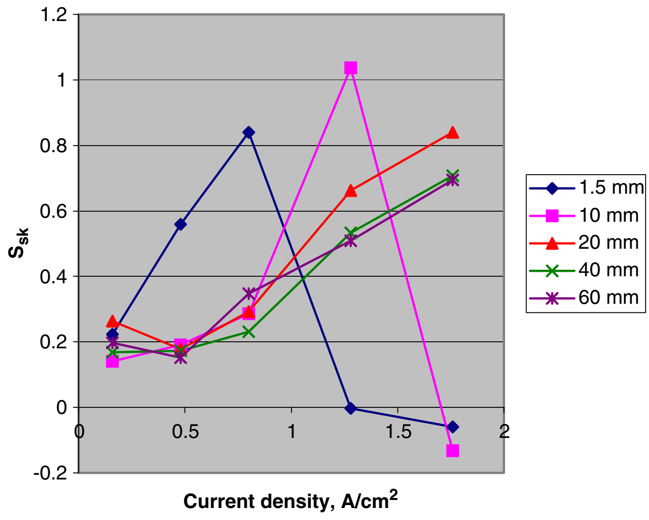

Fig. 19 Trends of S_{sk} with current density at different electrode gap levels

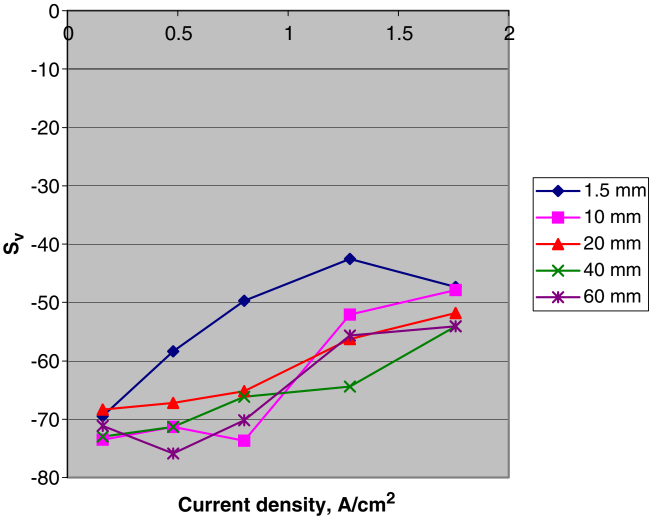

Fig. 21 Trends of S_v with current density at different electrode gap levels

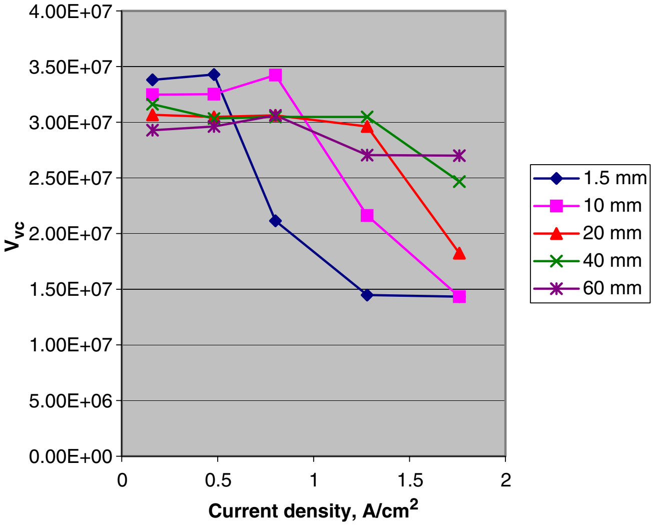

Fig. 22 Trends of V_{vc} with current density at different electrode gap levels

the V_{mc} parameter, the increasing trend of its magnitude with increase in the gap is very clear, especially at higher current density values. For the peak material volume, though a similar increasing trend is observed at the higher current density, there are some deviations in the data points, especially at 1.28 A/cm^2. The behaviour of V_{mp} at higher current density appears to be less predictable, and different phenomena such as polishing and etching might be taking place when the electrode gap is increased from 1.5 mm to 60 mm. From Fig. 16 a very low value of V_{mp} is observed for the small electrode gaps of 1.5 mm and 10 mm at the current density of 1.76 A/cm^2. Polishing action might be occurring under these conditions, whereas for the wider electrode gaps there appears to be a tendency for etching.

The reduction of the V_{mp} parameter at high current density and narrow electrode gap indicates that since S_q is small and S_{ds} is high, the numerous short summits have a less spiky topography. This is confirmed by the graphs of S_{ku} and S_{sk} with current density at different electrode gap levels (Figs. 18 and 19). From Fig. 18, with increasing current density, the value of S_{ku} tends to increase (and is above 3) indicating that there is a high frequency of occurrence of shorter peaks, and that the distribution of peaks' height is centrally distributed, i.e. very narrow.

The trend of S_{sk} (Fig. 19) for the narrow electrode gap conditions (1.5 mm and 10 mm) indicates that as the current density is increased from 0.16 A/cm^2 to 1.76 A/cm^2, there is a limiting condition of current density where a significant reduction (negative value) in the S_{sk} value is observed. For the 10 mm electrode gap this value stands at 1.28 A/cm^2 whereas for the 1.5 mm gap it is at 0.8 A/cm^2. The reduction of S_{sk} towards a negative value reveals that the resulting ECP surface is not dominated by spiky summits but rather flat summits with a few shallow outliers (such as troughs). If the outliers were of greater depth, then a larger negative skew would have resulted ($S_{sk}<-1$). However, with wider electrode gap, 20 mm and above, there is an increase in the S_{sk} value from 0.16 A/cm^2 to 1.76 A/cm^2. This would indicate that though the polishing action is taking place, the surface still has a few spikes. Thus a mild polishing effect is taking place even at a high current density (1.76 A/cm^2) for the wide electrode gaps and could be attributed to the longer path length for the ion's migration. For these electrode gaps, a high current density would be needed to have a higher polishing effect, that is, eradicating the spikes completely, and having shallow troughs.

When analysing the trend of the peak height (S_p) and that of the valley depth (S_v), a reduction (Figs. 20 and 21) is observed in both cases when the current density is increased (for all electrode gap levels). The same observation is made for the trend of the core valley (V_{vc}) and the void valley (V_{vv}) volume parameters (Figs. 22 and 23). All these findings show that as the polishing effect is progressing, the summits are decreasing in height, and flatten out so that the troughs become shallower and wider. This confirms the observation for the trend of S_{dr} where the

Fig. 23 Trends of V_{vv} with current density at different electrode gap levels

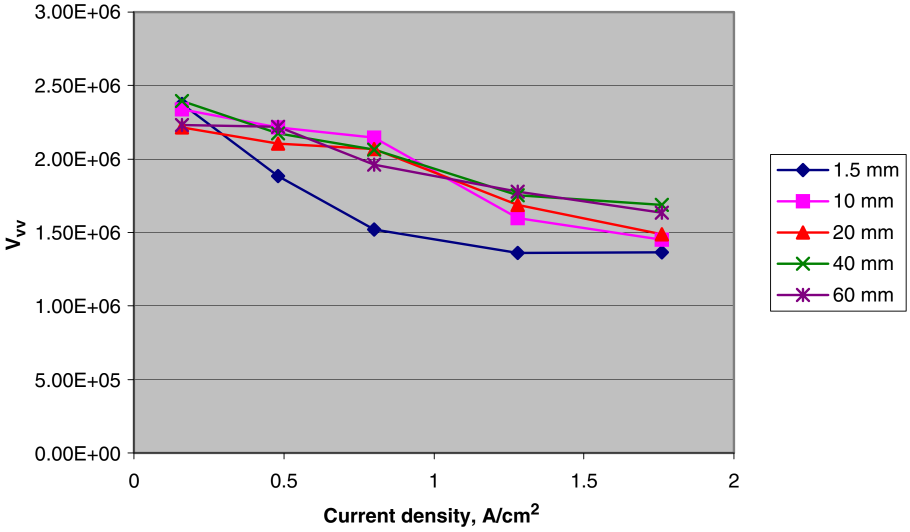

Table 4 3D surface texture data for medium/high current density and narrow gap conditions

3D parameter	ECP specimen number 11	12	16	17	21	22
S_q (μm)	17.71	25.91	11.94	18.02	12.02	12.21
S_z (μm)	153.33	187.67	87.06	145.33	93.56	100.20
S_{ds} (1/mm^2)	577.33	234.67	849.00	446.33	918.67	777.00
S_{tr}	0.64	0.85	0.85	0.85	0.91	0.86
S_{dr} (%)	9.22	18.93	8.96	9.15	12.09	5.37
V_{mp} (μm^3/mm^2)	1.44E+06	1.15E+06	5.58E+05	1.71E+06	5.49E+05	5.58E+05
V_{mc} (μm^3/mm^2)	1.44E+07	2.41E+07	1.06E+07	1.33E+07	1.08E+07	1.09E+07
V_{vc} (μm^3/mm^2)	2.12E+07	3.42E+07	1.45E+07	2.16E+07	1.43E+07	1.43E+07
V_{vv} (μm^3/mm^2)	1.52E+06	2.15E+06	1.36E+06	1.60E+06	1.37E+06	1.45E+06
S_{pk} (μm)	28.89	24.52	11.28	35.24	11.07	11.66
S_k (μm)	41.39	71.90	31.08	36.33	31.95	31.41
S_{5z} (μm)	144.00	175.00	85.63	140.00	89.37	96.92
S_a (μm)	13.48	21.34	9.50	13.19	9.63	9.69

risk of loss of dimensional fit of mating surfaces is minimum for surfaces produced under a high current density and its related optimum electrode gap.

Thus the appropriate selection of the current and electrode gap will provide a high value of the S_{ds} parameter while having a low S_q magnitude. This will ensure that the surface has a less spiky topography, which will definitely provide a better load carrying capacity.

Visual inspection of the surface of specimen ECP21 (1.76 A/cm^2 and 1.5 mm) revealed a less polished texture as compared to specimen ECP16 (1.28 A/cm^2 and 1.5 mm). At the higher current density (1.76 A/cm^2) and narrow gap (1.5 mm), random phenomena such as accumulation of precipitate might have caused a sparking condition, thereby leading to a partial pitting action on specimen ECP21.

When comparing the 3D surface texture parameters of specimens ECP12, ECP17 and ECP22, a significant increase is observed in the surface texture. ECP17 and ECP22 have been electrochemically polished with an electrode gap of 10 mm at 1.28 A/cm^2 and 1.76 A/cm^2, respectively; whereas ECP16 and ECP21 have been processed at an electrode gap of 1.5 mm but at the same current density as ECP17 and ECP22, respectively. ECP22 has a better surface texture as compared to ECP17 but ECP21 has suffered a slight deterioration as compared to ECP16. Moreover, comparison of the different 3D surface texture data for ECP16, ECP17, ECP21, and ECP22 are shown in Table 4. Each value represents the mean of three 3D measurements, and the deviation among these three measurements is in the range of 8–15%. It can be seen that the best result was obtained on specimen ECP16, where the current density was set at 1.28 A/cm^2 with the minimum electrode gap (1.5 mm). This combination is better than the case where a current of 1.76 A/cm^2 at a gap of 10 mm confirms the strong interaction effect of the two factors, which was observed from the ANOVA results. Indeed, the ANOVA results have shown that for many 3D surface texture parameters, the interaction effect of the two factors was higher than the individual effect of the electrode gap.

From Figs. 24 and 25 it can be seen that the surface flaws on ECP21 are much wider and bigger than that on ECP16.

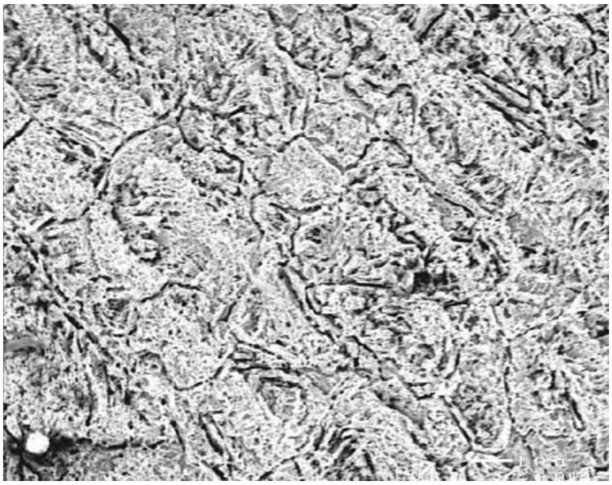

Fig. 24 Electropolished specimen ECP16 (1.28 A/cm^2 and 1.5 mm) at magnification = 750X

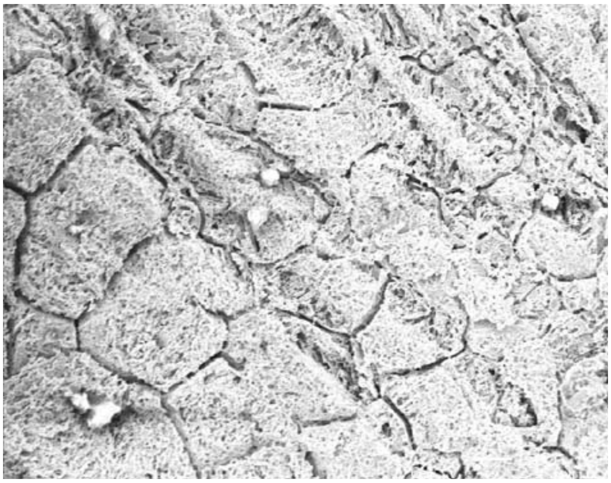

Fig. 25 Electropolished specimen ECP21 (1.76 A/cm^2 and 1.5 mm) at magnification = 750X

The flaws might be due to some preferential etching at grain boundaries or at regions where there is higher presence of alloying elements or even due to discontinuities in the microstructure. These SEM pictures tend to show that the surface produced by the lower current density, i.e. at 1.28 A/cm^2 (ECP16), is better than that at 1.76 A/cm^2 (ECP21), given that both have the same electrode gap (1.5 mm). This finding confirms the 3D surface texture results, whereby the amplitude as well as the volume parameters (such as V_{vc} and V_{mc}) were found slightly increased when the current density was increased from 1.28 A/cm^2 to 1.76 A/cm^2.

6 Conclusion

The preliminary set of electrochemical polishing tests has revealed that the current and electrode gap have a higher influence on the surface improvement of the EDM specimens as compared to the flow rate of the electrolyte.

The 3D surface analysis results of the final set of ECP tests have shown that current density has a higher influence on the 3D surface roughness parameters. Furthermore, a high contribution due to the current density-interelectrode gap interaction was observed. For a given current density level, there is an optimum value of interelectrode gap at which the maximum surface improvement is achieved. If a smaller interelectrode gap is used, then there is the risk of random phenomena such as sparking taking place, thereby damaging the surface. This phenomenon was observed both from the data obtained by the 3D surface characterisation and scanning electron microscope analysis.

The 3D surface texture parameters have shown the influence of the variation of the ECP process parameters, and have revealed the importance of 3D measurement in understanding the functionality aspects of surfaces. Thus by properly selecting the process conditions, surfaces can be engineered so as to meet specific functional requirements. For example, significant polishing might be done to obtain a high value of S_{ds} and low values of S_{dr} and volume parameters but this component might not be subjected to a dynamic situation, and therefore the issues of improved load bearing capability and running in wear do not arise. This will also ensure that the cost associated with the development of a surface is optimised.

Acknowledgements One of the authors (H. Ramasawmy) is grateful to the United States government for having provided funding (Fulbright Scholarship Scheme) for the research attachment, and also to the University of Nebraska-Lincoln, in particular the Non Traditional Research Center, for all the facilities made available. This author is also thankful to Professor V.C. Oleti for his kind views and suggestions on the paper.

References

1. McGeough JA, Khayry ABM, Munro W (1983) Theoretical and experimental investigation of the relative effects of spark erosion and electrochemical dissolution in electrochemical arc machining. CIRP Ann 32(1):113–118
2. Sakai S, Masuzawa T, Ito S (1989) ECM finishing of surface products by EDM. Proceedings of international symposium on electromagnetic metrology (ISEM 89), 19–22 August, Beijing, China, vol 9, pp 155–158
3. Boza P (1997) Contribution a l'augmentation de l'Efficacite de Coupe des Outils en Acier Rapide par Polissage Electrochimique. PhD Thesis, Ecole Centrale de Paris, France, p 112
4. American Society of Metals (1964) Metals handbook: heat treating, cleaning and finishing, vol 2, 8th edn. Metals Park, Ohio, pp 484–488
5. Lilly BW, Brevick J (1997) The effect of pulsed electrochemical machining on the fatigue life of H-13 steel. Trans North Am Manuf Res Inst SME 25:153–158
6. Lee ES (2000) Machining characteristics of the electropolishing of stainless steel (ST316L). Int J Adv Manuf Technol 16 (8):591–599
7. Jeyashree G, Subramanian A, Vasudevan T, Mohan S, Venkatachalam R (2000) Electropolishing of stainless steel. Bull Electrochem 16(9):388–391
8. Rajurkar KP, Schnacker CL (1988) Some aspects of ECM performance and control. CIRP Ann 37(1):183–186
9. Masuzawa T, Sakai S (1987) Quick finishing of WEDM products by ECM using a mate-electrode. CIRP Ann 36 (1):123–126
10. Blunt L, Ebdon S (1996) The application of three-dimensional surface measurement techniques to characterizing grinding wheel topography. Int J Mach Tools Manuf 36(11):1207–1226
11. Blunt L, Jiang X, Stout KJ (1999) Developments in 3D surface metrology. Proceedings of the international conference on laser metrology and machine performance (Lambdamap), Newcastle, UK
12. Blunt L, Wang K, Stout KJ (1998) *Ballising* - a technique for surface engineering. Workshop on engineered surfaces, Corps, France
13. Stout KJ, Blunt L (1995) Application of 3D topography to bioengineering. Int J Mach Tools Manuf 35(2):219–229
14. Stout KJ, Blunt L (1995) Nanometres to micrometres: three-dimensional surface measurement in bio-engineering. J Surf Coat Technol 71:69–81
15. Stout KJ, Sullivan PJ, Dong WP, Mainsah E, Luo N, Mathia T, Zahouani H (1993) The development of methods for the characterisation of roughness in three dimensions. Penton Press, London, pp 217–246